

Casein nanoparticles in combination with 2-hydroxypropyl- β -cyclodextrin improves the oral bioavailability of quercetin

Rebeca Peñalva, Irene Esparza, Jorge Morales, Carlos J. González-Navarro, Eneko Larrañeta, Juan M. Irache*

Department of Chemistry and Pharmaceutical Technology, NANO-VAC Research Group, University of Navarra, Spain

***Corresponding author:**

Prof. Juan M. Irache
Dep. Chemistry and Pharmaceutical Technology
NANO-VAC Research Group
University of Navarra
C/ Irunlarrea, 1
31008 – Pamplona
Spain
Phone: +34948425600
Fax: +34948425619
E-mail: jmirache@unav.es

© 2019 Elsevier B.V.

This manuscript version is made available under the CC-BY-NC-ND 4.0 license
<http://creativecommons.org/licenses/by-nc-nd/4.0/>

Rebeca Peñalva, Irene Esparza, Jorge Morales-Gracia, Carlos J. González-Navarro, Eneko Larrañeta, Juan M. Irache, Casein nanoparticles in combination with 2-hydroxypropyl- β -cyclodextrin improves the oral bioavailability of quercetin, *International Journal of Pharmaceutics*, Volume 570, 2019, 118652, ISSN 0378-5173, <https://doi.org/10.1016/j.ijpharm.2019.118652>.

Abstract

The aim of this work was to optimize the preparative process of quercetin loaded casein nanoparticles as well as to evaluate the pharmacokinetics of this flavonoid when administered orally in Wistar rats. Nanoparticles were obtained by coacervation after the incubation of casein, 2-hydroxypropyl- β -cyclodextrin (HP- β -CD) and quercetin in an aqueous environment. Then, nanoparticles were purified and dried. The resulting nanoparticles displayed a size of 200 nm with a negative zeta potential and a payload of about 32 μ g/mg. Release studies showed a zero-order kinetic, suggesting a mechanism based on erosion of the nanoparticle matrix. For the pharmacokinetic study, quercetin was orally administered to rats as a single dose of 25 mg/kg. Animals treated with quercetin-loaded casein nanoparticles displayed higher plasma levels than those observed in animals receiving the solution of the flavonoid (control). Thus, the relative oral bioavailability of quercetin when administered as casein nanoparticles (close to 37%) was found to be about 9-times higher than the oral solution of the flavonoid in a mixture of PEG 400 and water. In summary, the combination of casein and 2-hydroxypropyl- β -cyclodextrin produces nanoparticles that may be a good option to load quercetin for both nutraceutical and pharmaceutical purposes.

Key words: nanoparticles; cyclodextrin; casein; quercetin; nutraceutical; oral delivery

1. Introduction

Quercetin (3,3',4',5,7-pentahydroxyflavone) is a naturally occurring flavonoid and one of the most potent antioxidants of plant origin (Anand David et al., 2016; Zhang M. et al., 2011). Chronic intake of quercetin may be associated with a decreased risk of coronary heart disease (Patel et al., 2018; Perez-Vizcaino et al., 2006) and other degenerative conditions, including cancer (Kashyap et al., 2016; Rauf et al., 2018), diabetes (Bule et al., 2019; Chen et al., 2016), and neurodegenerative disorders (Barreca et al., 2016; Dajas et al., 2015). The median daily intake of quercetin within a typical Western diet has been estimated as about 10 mg and the major sources would be tea, red wine, fruits, and vegetables (Egert et al., 2018). In some countries, quercetin is available as a dietary supplement with recommended daily doses ranging from 200 to 1200 mg (Harwood et al., 2007). In a similar way, it has been proposed the use of quercetin as a nutraceutical for functional foods within a concentration range of 10–125 mg/serving (Harwood et al., 2007; Russo et al., 2012).

However, when orally administered, quercetin shows a very low bioavailability (less than 10% in rats, 4% in dogs and even 1% in humans) (Khaled et al., 2003; Reinboth et al., 2010). This drawback would be related to the low solubility of the aglycone form (around 10 mg/L in water) (Smith et al., 2011) as well as to the intense presystemic metabolism suffering by this flavonoid in the gut mucosa. In fact, quercetin would be substrate of the efflux pumps (e.g., intestinal P-glycoprotein) and cytochrome P-450 (CYP) isoenzymes and transferases located both in the gastrointestinal tract and in the liver (Babu et al., 2013; Limtrakul et al., 2005; Wang et al., 2014). As a result of this metabolism, the glucuronide and sulphate derivatives of quercetin would be the major circulating compounds in plasma (Lodi et al., 2009; Nakamura et al., 2018). Apart from its considerable metabolism, quercetin is chemo- and thermo-labile and rapidly degraded when exposed to alkaline media, light or warm temperature (Scalia and Mezzena, 2009).

In order to enhance the oral bioavailability of quercetin, different strategies have been tested, including the synthesis of analogues of the flavonoid (Iacopetta et al., 2017; Kim et al., 2009) and the co-administration with P-gp inhibitors (i.e., piperine) (Rinwa and Kumar, 2017). In a similar way, the use of nanocarriers has been suggested to promote the oral absorption of quercetin. Some authors have proposed, inter alia, nanosuspensions (Gao et al., 2011), self-emulsifying delivery systems (Jain et al., 2014), nanoemulsions (Karadag et al., 2013), liposomes (Caddeo et al., 2019), and nanoparticles (de Oliveira Pedro et al., 2018; Li et al., 2009; Moreno et al., 2017).

Another interesting alternative would be the use of casein-based nanoparticles. These nanoparticles can be prepared by a simple coacervation process, in an aqueous environment without using any type of organic solvent or toxic reagent (Penalva et al., 2015). The resulting nanoparticles show a certain capability to reach the epithelium surface of the gut mucosa (Peñalva et al., 2018), facilitating the absorption of the loaded compound. Moreover, casein is the main protein in raw milk (about 80%) and one of the most commonly used by the industry for supplementation purposes (Hoffman and Falvo, 2004). This fact would facilitate the use of casein-based nanoparticles to develop pharmaceutical and nutraceutical products or functional foods.

Therefore, the aim of this work was to optimize the preparative process of quercetin-loaded casein nanoparticles as well as to evaluate their capabilities to promote the oral absorption and bioavailability of quercetin in Wistar rats. In this context, and in order to

minimize the pre-systemic metabolism of quercetin, 2-hydroxypropyl- β -cyclodextrin was associated with casein nanoparticles in order to disturb the effect of both the intestinal efflux pumps and the cytochrome P450 enzymatic complex (Buggins et al., 2007; Takizawa et al., 2013; Zhang Y. et al., 2011).

2. Materials and methods

2.1. Reagents

Sodium caseinate was obtained from ANVISA (Madrid, Spain). Quercetin, lysine, 2-hydroxy-propyl- β -cyclodextrin (HP- β -CD), mannitol, chlorzoxazone, calcium chloride, poly(ethylene glycol) 400 (PEG 400), and tween 20 were from Sigma-Aldrich (Germany). Ethanol, methanol, acetic acid and acetonitrile (HPLC grade) were from Merck (Darmstadt, Germany). All reagents and chemicals used were of analytical grade.

2.2. Preparation of quercetin-loaded casein nanoparticles

Nanoparticles were prepared by simple coacervation procedure followed by a purification step by ultrafiltration and subsequent drying by Spray-drying (Penalva et al., 2015).

Briefly, 1 g sodium caseinate, 90 mg lysine (as stabilizer (Penalva et al., 2015)) and a variable amount of HP- β -CD were dissolved in 75 mL purified water. In parallel, 35 mg quercetin were dissolved in 3 mL absolute ethanol and added under magnetic stirring to the casein solution. Under magnetic stirring, nanoparticles were formed by the addition of 40 mL of an aqueous solution of calcium chloride 0.8% w/v. The resulting suspension was purified by ultrafiltration through a polysulfone membrane cartridge of 50kDa pore size (Medica SPA, Italy). Finally, 30 mL of an aqueous solution of mannitol (100 mg/mL) were added to the suspension of casein nanoparticles and the mixture was dried in a Buchi Mini Spray Drier B-290 apparatus (BuchiLabortechnik AG, Switzerland) under the following experimental conditions: (i) inlet temperature: 90°C, (ii) outlet temperature: 45-50°C, (iii) air pressure: 2-5 bar, (iv) pumping rate: 2-6 mL/min, (v) aspirator: 100% and (vi) air flow: 900 L/h. The resulting nanoparticles were named Q-HPCD-NP.

On the other hand, nanoparticles in the absence of the cyclodextrin were also prepared (Q-NP). In this case, sodium caseinate (1 g), lysine (90 mg) and an ethanol solution of quercetin (35 mg in 3 mL) were dissolved in 75 mL purified water. Then, nanoparticles were obtained by the addition of 40 mL of a solution of calcium chloride in purified water (0.8% w/v). The resulting nanosuspensions were purified and dried as described above. Empty nanoparticles were also prepared as described above but either in the absence of the oligosaccharide and quercetin (NP) or in the absence of the flavonoid (HPCD-NP).

2.3. Preparation of quercetin conventional formulations

For in vivo studies, two conventional formulations of quercetin were used. The first consisted on a solution of the polyphenol in a mixture of PEG 400 and water (6:4 by vol.). For this purpose, 62.5 mg quercetin were dissolved in 6 mL PEG 400 under magnetic stirring. Then 4 mL purified water were added and the final mixture was agitated in darkness conditions for 10 min. This formulation was identified as Q-sol.

The second formulation was an extemporaneous suspension of quercetin in purified water (Q-susp). Briefly, 62.5 mg quercetin was dispersed in 10 mL purified water under

magnetic agitation for 10 min. The size of the resulting suspension was $15.5 \pm 4.3 \mu\text{m}$. The suspension was used after inspection for absence of aggregates.

2.4. Characterization of nanoparticles

2.4.1. Size, zeta potential and morphology

The mean hydrodynamic diameter and the zeta potential of nanoparticles were determined by photon correlation spectroscopy (PCS) and electrophoretic laser Doppler anemometry, respectively, using a Zetaplus apparatus (Brookhaven Instrument Corporation, USA). The diameter of the nanoparticles was determined after dispersion in ultrapure water (1:10) and measured at 25°C with a scattering angle of 90°. The zeta potential was measured after dispersion of the dried nanoparticles in 1 mM KCl solution. The morphology and shape of nanoparticles was examined using a field emission scanning electron microscope (FE-SEM) in a Zeiss DSM940 digital scanning electron microscope (Oberkochen, Germany) coupled with a digital image system (Point Electronic GmbH, Germany). Prior to the microscopy analysis, particles were washed to remove mannitol. For this purpose, spray-dried nanoparticles were resuspended in distilled water and centrifuged at 27,000 x g for 10 min. Then, the supernatants were discarded and the pellets were mounted on copper grids. Finally, the pellet was shaded with an amalgam of gold/palladium for fifteen seconds using a sputter coater (K550X Emitech, Ashford, UK).

The yield of the process was calculated by gravimetry as described previously (Peñalva et al., 2018).

2.4.2. Quercetin analysis

The amount of quercetin loaded into the nanoparticles was quantified by HPLC-UV following an analytical method previously published with minor modifications (Iacopini et al., 2008). Analysis were carried out in an Agilent model 1100 series LC and a diode-array detector set at 370 nm. The chromatographic system was equipped with a reversed-phase 150 mm x 2.1 mm C18 Alltima column (particle size 5 μm ; Altech, USA) and a Gemini C18 precolumn (particle size 5 μm ; Phenomenex, CA, USA). The mobile phase, pumped at 0.25 mL/min, consisted of a mixture of methanol, water and acetic acid in gradient conditions. The column was placed at 40°C and the injection volume was 10 μL . Calibration curves were designed over the range of 0.3-100 $\mu\text{g}/\text{mL}$. The limit of quantification was calculated to be 0.35 $\mu\text{g}/\text{mL}$.

For analysis, 10 mg nanoparticles were dispersed in 1 mL water and centrifuged at 30,500 xg for 20 min. The supernatants were analyzed in order to determine the amount of free quercetin (not encapsulated). The amount of quercetin loaded in the nanoparticles was calculated by subtracting from the theoretical amount of quercetin, the amount of drug found in the supernatant (equation 1). The encapsulation efficiency (EE) was calculated with equation 2. Each sample was assayed by triplicate and the results were expressed as the amount of quercetin (in μg) per mg nanoparticles.

$$\text{Quercetin loaded } (\mu\text{g}/\text{mg}) = (Q_t - Q_s) / W_p \quad [\text{Eq. 1}]$$

$$\text{EE } (\%) = ((Q_t - Q_s) / (Q_t)) \times 100 \quad [\text{Eq. 2}]$$

in which Q_t is the total theoretical amount of quercetin in the formulations, Q_s corresponds to the amount of quercetin quantified in the supernatants and W_p the amount of protein quantified as described above.

2.5. In vitro release studies

Release experiments were conducted at 37°C using simulated gastric (SGF, pH 1.2) and intestinal (SIF, pH 6.8) fluids (European Pharmacopoeia, 2013). In order to fulfil sink conditions, Tween® 20 (0.5% w/v) was added to both media. The studies were performed under agitation in a slide-A-Lyzer® Dialysis cassette 10.000 MWCO (Thermo scientific, Rockford, IL, USA).

For the study, 2 mg of quercetin loaded in casein nanoparticles were dispersed in 5 mL of purified water and introduced in the cassette, which was then placed into a vessel containing 500 mL of SGF for 2 hours. After this time, the same cassette was removed from the SGF and introduced in a second vessel with 500 mL SIF until the end of the experiment. At different time points, samples of 1 mL were collected and filtered to 0.45 µm (Filter nylon, Thermo scientific, Rockford, USA) before quantification. At each sampling time, the withdrawn volume was replaced with fresh fluid (gastric or intestinal simulated fluids).

The amount of quercetin released from the formulations was quantified by HPLC. Calibration curves of quercetin were prepared in both release media over the range of 0.16-6 µg /mL ($R^2 > 0.99$).

2.5.1. Analysis of release data

In order to ascertain the drug release mechanism, data obtained from the in vitro release experiments were fitted to Korsmeyer-Peppas and zero-order models. The Korsmeyer-Peppas model (Ritger and Peppas, 1987) is a simple semi-empirical model which exponentially relates drug release with the elapsed time (equation 3).

$$M_t/M_\infty = K_{KP} t^n \quad [\text{Eq. 3}]$$

Where M_t/M_∞ is the drug release fraction at time t , K_{KP} is a constant incorporating the structural and geometric characteristics of the matrix and n is the release exponent indicative of the drug release mechanism. The value of "n" indicates the mechanism of the release (Ritger and Peppas, 1987). If the value is around 0.5, the mechanism is Case I (Fickian) diffusion, and a value between 0.5 and 0.89 indicates anomalous (non-Fickian) diffusion suggesting a combination of mechanisms diffusion and erosion. Values of "n" between 0.89 and 1 indicate Case II transport, which involves a release mechanism ruled by erosion/relaxation of the matrix.

Data obtained from the in vitro release experiments were also fitted to a zero-order kinetic equation (equation 4). This model is used for systems where the matrix releases the same amount of drug by unit of time (Costa and Sousa Lobo, 2001).

$$M_t/M_\infty = K_{ZO} t \quad [\text{Eq. 4}]$$

Where M_t/M_∞ is the drug release fraction at time t , and K_{ZO} is the zero order release constant.

To fit the experimental data to the previous equation, only one portion of the release profile was used, that is $M_t/M_\infty \leq 0.6$ (Costa and Sousa Lobo, 2001).

2.6. In vivo pharmacokinetic studies in Wistar rats

Pharmacokinetic studies were performed in male Wistar rats (200-250 g) obtained from Harlan (Barcelona, Spain). Studies were approved by the Ethical Committee for Animal Experimentation of the University of Navarra (protocol number 028-11) in accordance with the European legislation on animal experiments. Before the oral administration of the formulations, animals were fasted overnight to avoid interference with the absorption, allowing free access to water.

For the pharmacokinetic study, rats were randomly divided into 5 groups (n=6). The experimental groups were as follows: (i) quercetin aqueous suspension (Q-susp), (ii) quercetin solution in PEG 400:water (60:40 v/v) (Q-sol) (iii) quercetin-loaded casein nanoparticles (Q-NP) and (iv) quercetin-loaded casein nanoparticles containing HP- β -CD (Q-HPCD-NP). All of these formulations were orally administered with a blunt needle via into the stomach. As control, a group of animals received intravenously the solution of quercetin in the mixture of PEG 400 and water. In all cases, the dose of quercetin (orally or intravenously) was 25 mg/kg body weight.

Blood samples were collected at set times after administration (0, 10 min, 30 min, 1, 2, 4, 6, 8, 24 and 48 hours) in Microvette® 500K3E plasma tubes (SARSTEDT, Germany). Blood volume was recovered intraperitoneally with an equal volume of normal saline solution pre-heated at body temperature. Samples were immediately centrifuged at 9,400 x g for 10 min and plasma aliquots were frozen at -80 °C until analysis.

2.6.1. Determination of quercetin plasma concentration

The amount of quercetin was determined in plasma by HPLC as described above using chlorzoxazone as internal standard. Prior the analysis, quercetin was extracted from plasma samples following a protocol previously described by Li and co-workers (Li et al., 2009) with minor modifications. For sample preparation, an aliquot of 100 μ L plasma sample was mixed with 25 μ L internal standard solution (chlorzoxazone, 50 μ g/mL in methanol), 125 μ L methanol and 50 μ L HCl (25% by vol.) for protein precipitation followed by vigorous shaking at 2500 rpm for 10 min. Then, samples were hydrolyzed in a water bath at 50°C for 15 min and were centrifuged at 10,000 rpm for 10 min. The obtained supernatants were filtered (Filter nylon, 0.45 μ L, Thermo scientific, Rockford, USA) and a 50 μ L aliquot of each sample were injected onto the HPLC column.

The same protocol was used for calibration and quality control standards preparation, using blank plasma and different solutions of quercetin in methanol. Calibration curves were designed over the range 70-5000 ng/mL ($R^2 > 0.999$). Under these experimental conditions, the run time of quercetin was 13.9 min (detected at 370 nm) and the internal standard 12.6 min (detected at 303 nm). The limit of quantification was calculated as 200 ng/mL. Linearity, accuracy and precision values during the same day (intraday assay) at low, medium and high concentrations of quercetin were within the acceptable limits (relative error and coefficient of variation less than 15%).

2.6.2. Pharmacokinetic data analysis

Quercetin plasma concentration was plotted against time, and pharmacokinetic analysis, was performed using a non-compartmental model with the WinNonlin 5.2 software (Pharsight Corporation, USA). The following parameters were estimated: maximal serum concentration (C_{max}), time in which C_{max} is reached (T_{max}), area under the concentration-time curve from time 0 to last time (AUC), mean residence time (MRT), clearance (Cl), volume of distribution (V) and half-life in the terminal phase ($t_{1/2}$).

Furthermore, the relative bioavailability (Fr) of quercetin was estimated by the following equation:

$$\text{Fr (\%)} = (\text{AUC}_{\text{oral}})/(\text{AUC}_{\text{iv}}) \times 100 \quad [\text{Eq. 5}]$$

Where AUC_{iv} and AUC_{oral} are the areas under the curve for the intravenous and oral administrations, respectively.

2.7. Statistical analysis

Data are expressed as the mean \pm standard deviation (SD) of at least three experiments. The non-parametric Kruskal-Wallis followed by Mann-Whitney U-test was used to investigate statistical differences. In all cases, $p < 0.05$ was considered to be statistically significant. All data processing was performed using Graph Pad® Prism statistical software.

3. Results

3.1. Optimization and preparation of quercetin-loaded nanoparticles

For the optimization of the preparative process of quercetin-loaded nanoparticles, the flavonoid-to-cyclodextrin ratio and the time of incubation between the main components of the formulation (sodium caseinate, quercetin and HP- β -CD) before the formation of nanoparticles were evaluated. Figure 1 shows the influence of the incubation time and the quercetin-to-HP- β -CD ratio on the encapsulation efficiency and payload of the resulting nanoparticles. The highest loading was obtained with a time of incubation of 30 min (between the components of the formulation) and quercetin-to-HP- β -CD ratios of either 1:1 or 1:2 by mol. Under these experimental conditions, the payload of the resulting nanoparticles was about 31 μg quercetin per mg nanoparticles with an encapsulation efficiency higher than 80%. Thus, the following experimental conditions were selected: a quercetin-to-cyclodextrin ratio of 1:1 by mol and a time of incubation of 30 minute.

Table 1 summarises the main physico-chemical characteristics of the nanoparticles used in this study. The mean diameter of empty casein nanoparticles was smaller than those loaded with quercetin. On the other hand, the incorporation of HP- β -CD decreased the mean diameter of the quercetin-loaded nanoparticles from 251 nm (for Q-NP) to 171 nm (for Q-HPCD-NP). In all cases, the polydispersity index was below 0.3, indicating homogeneous nanoparticle formulations, and the zeta potential was negative. This negative charge was slightly higher when quercetin was loaded in casein nanoparticles. Another important aspect to highlight was that the incorporation of HP- β -CD increased 40% the quercetin loading in casein nanoparticles (22.3 $\mu\text{g}/\text{mg}$ vs. 31.5 $\mu\text{g}/\text{mg}$).

The morphological analysis by scanning electron microscopy (Figure 2) showed that quercetin-loaded casein nanoparticles consisted of homogeneous population of irregular shaped nanoparticles, with a mean size similar to that obtained by photon correlation spectroscopy. Q-NP (Figure 2A) displayed a smooth surface; however, the formulation containing the cyclodextrin displayed nanoparticles with a rough surface (Figure 2B).

3.2. In vitro release profile

The release of quercetin from casein nanoparticles was evaluated in simulated gastric and intestinal fluids (Figure 3). Overall, the release of quercetin appeared to be independent of the pH conditions and slightly more rapid when released from Q-NP than from Q-HPCD-NP. For the first 2 hours, under SGF, about 20% of the loaded quercetin was released from both nanoparticle formulations. Then, after 4 hours of incubation in SIF, the amount of quercetin released was around 80% of the total content in Q-NP and close to 60% from Q-HPCD-NP. In any way, from both nanoparticle formulations, 24 hours after the beginning of the experiment, almost the total amount of the encapsulated quercetin was released from casein nanoparticles.

The quercetin release data from both nanoparticles were fitted to the Korsmeyer-Peppas model, obtaining “n” values close to 1 (Table 2). These data suggested that the quercetin release from nanoparticles involves a release mechanism ruled by an erosion/relaxation phenomenon of the matrix. The release data were fitted to the zero-order model, obtaining good regression coefficients ($r^2 > 0.98$). In all cases, the release constants were slightly higher when quercetin was released from nanoparticles prepared in the absence of HP- β -CD than from Q-HPCD-NP.

3.3. Pharmacokinetic study

Figure 4 shows the plasma concentration-time profile of quercetin after the oral administration of a single dose in rats (25 mg/kg) formulated as solution in a mixture of PEG400 and water (60:40 by vol.), aqueous suspension or encapsulated in casein nanoparticles. From the oral administration of the aqueous solution (Q-sol), the quercetin levels in the plasma of animals increased rapidly during the first hour post-administration when the C_{max} was reached. Then, the amount of quercetin in plasma decreased slowly during the following hours. For the aqueous suspension (Q-susp), the plasma levels of the flavonoid were quite low and quercetin was only quantified in plasma during the first 4 hours post-administration. On the contrary, for nanoparticle formulations (Q-NP and Q-HPCD-NP), quercetin plasma levels were significantly higher and more sustained and prolonged in time than those observed for the conventional formulations (Q-sol and Q-susp). For Q-NP, these high levels of the flavonoid in plasma were quantified up to 24 hours post-administration, whereas, for Q-HPCD-NP, plasma levels were observed up to 72 hours post-administration.

For comparative purposes and pharmacokinetic analysis, the PEG-water solution of quercetin was also iv administered (25 mg/kg). In this case, the data adjusted well to a non-compartmental model characterized by a rapid decrease in a biphasic way of quercetin plasma concentrations. Moreover, 8-h post administration, quercetin in plasma was no longer quantified (data not shown).

Table 3 summarizes the pharmacokinetic parameters estimated during the analysis of the experimental data obtained after the administration of the different quercetin formulations to rats. The oral solution of quercetin provided an AUC value 10-times higher than that observed for the suspension of the flavonoid (Q-susp). For classical casein nanoparticles (Q-NP), the AUC value was about 3-times higher than for the oral solution of the flavonoid. Moreover, for Q-HPCD-NP, the AUC was the highest and represented 61 $\mu\text{g h/mL}$, about 10-fold higher than the value calculated for the oral solution of quercetin. The half-life and the mean residence time of quercetin in plasma were significantly higher when the flavonoid was administered in casein nanoparticles than formulated as solution or suspension. In a similar way, the volume of distribution

of quercetin also increased when the flavonoid was encapsulated in casein nanoparticles, whereas its clearance was of the same order in all cases. Finally, the relative oral bioavailability of quercetin when incorporated in casein nanoparticles ranged from 11% to 36% (for Q-NP and Q-HPCD-NP, respectively). However, for the oral solution, the oral bioavailability of the flavonoid was only of about 4%.

4. Discussion

Quercetin, due to its beneficial effects, has been proposed as an interesting compound for dietary supplementation and food fortification (Aherne and O'Brien, 2002; Dwyer et al., 2015; Lin et al., 2019). However, due to its low oral bioavailability, formulation alternatives are necessary to solve this drawback. Nanoencapsulation may be an interesting approach to both improve the absorption of the loaded compound and offer protection against degradation or inactivation during storage and/or after administration. Regarding food fortification (process of adding nutrients or bioactive components to edible products (Dwyer et al., 2015)), the material employed to produce these nanoparticles should be GRAS and, ideally, to be a constituent of the food matrix. Among others, milk-based products are considered as good vehicles for bioactive components because they are staple food for a large part of the population (Ganesan et al., 2014; Karam et al., 2013). In this context, casein-based nanoparticles would be appropriate carriers for fortification of dairy products.

In our study, casein nanoparticles were prepared by a simple coacervation method followed by a purification step and a subsequently drying process in order to minimize the physico-chemical degradation of the flavonoid. The mean size of the quercetin-loaded casein nanoparticles was about 170 nm with a zeta potential of -15 mV. Interestingly, the incorporation of HP- β -CD produced more homogeneous (decreased PDI, Table 1) and smaller nanoparticles, without affecting their surface negative charge properties. Furthermore, the incorporation of the oligosaccharide permitted us to significantly increase the quercetin loading (31 μ g/mg vs. 22 μ g/mg in the absence of the cyclodextrin). This payload is in line with other previous results reported by other authors using similar devices such as Eudragit[®] L (acrylic polymer) nanoparticles (Pool et al., 2012), PLGA nanocapsules (Ghosh et al., 2011) or solid lipid nanoparticles (Li et al., 2009).

On the other hand, the release of quercetin from casein nanoparticles appeared to be independent of the pH conditions and followed a zero-order kinetic. This fact could be explained by the entry of the aqueous medium inside the casein nanoparticles that induced the diffusion of quercetin by a release mechanism ruled by erosion/relaxation of the matrix. Surprisingly, the incorporation of the cyclodextrin to the casein nanoparticles slightly decreased the release rate of quercetin from the resulting nanocarriers. This finding would suggest that the oligosaccharide interacts with casein to form a more compact matrix that would delay the release of quercetin from nanoparticles. Some years ago, it was reported that β -cyclodextrin is capable of forming inclusion complex with β -casein (Lee and Fennema, 1991), and, thus, prevent its aggregation when warmed. In the same line, cyclodextrins have been proposed as stabilizers of therapeutic proteins in order to minimize aggregation phenomena (Serno et al., 2011). However, in this case, the interaction between the oligosaccharide molecules and the protein would yield to a compact and more resistant matrix to the

erosion and/or relaxation that would occur in an aqueous environment. In any case, further investigations are necessary to elucidate the real mechanism of the interaction between cyclodextrin and casein in the nanoparticulate form.

When quercetin was administered by the intravenous route as a solution of PEG400 and water, the profile of the curve was biphasic and similar to that published previously (Chen et al., 2005). The terminal half-life ($t_{1/2}$) of the quercetin was 0.6 h and the MRT was calculated to be 1.57 h. The oral administration of the same solution of quercetin induced discrete plasma levels that were only quantified during the first 8 hours post-administration. For this solution, the bioavailability of quercetin was calculated to be about 4%. This result is in line with the data obtained by Chen and co-workers, who described a quercetin bioavailability of 5% with a 15% HP- β -CD aqueous solution of the flavonoid in male Sprague-Dawley rats (Chen et al., 2005). When quercetin was loaded in nanoparticles and orally administered to rats, the plasma levels of the flavonoid were higher than those observed for the control oral formulations (Figure 4). The incorporation of HP- β -CD in casein nanoparticles produced a significant prolongation of the quercetin plasma levels up to 72 h. This result was also evidenced by the high half-life ($t_{1/2}$) and MRT of the flavonoid when administered in the casein nanoparticles (see Table 3). Under these circumstances, the relative oral bioavailability of quercetin was calculated to be close to 37% (nine times higher than for the control solution of the flavonoid). These prolonged and high levels of quercetin in plasma would be related to a combination of two phenomena. First, casein nanoparticles would conduct the cargo until the surface of the gut epithelium. The mucus-permeating properties of these carriers would facilitate both their arrival to the surface of the enterocytes and an increased residence time in close contact with the absorptive membrane. Second, the cargo would be released and the presence of HP- β -CD would disarm the intestinal efflux pumps and the enzymatic complex associated to the cytochrome P450 (Buggins et al., 2007; Ishikawa et al., 2005; Takizawa et al., 2013; Zhang Y. et al., 2011). All together would permit the absorption of quercetin and its improved bioavailability when encapsulated in these casein nanoparticles. Alternatively, lymphatic absorption may be a supplementary factor that can also contribute to this improved bioavailability observed for quercetin (aglycone) when loaded in casein nanoparticles. Recently, it has been demonstrated that quercetin may be absorbed by both intestinal capillaries and lymphatic ducts (Chen et al., 2010; Murota and Terao, 2005). This is important because absorption via the lymphatic system avoids hepatic first-pass metabolism and would prolong the presence of the flavonoid in the body.

5. Conclusions

In summary, the preparation of casein nanoparticles in the presence of HP- β -CD appears to be a good option to load quercetin for both nutraceutical and pharmaceutical purposes. The resulting nanoparticles offer a zero-order release rate of the flavonoid when incubated in simulated fluids. In vivo, these casein nanoparticles produced high and sustained levels of quercetin for periods up to 72 hours and an oral relative bioavailability close to 37%.

Acknowledgements

This work was supported by the Regional Government of Navarra (Alimentos funcionales, Euroinnova call) and the Spanish Ministry of Science and Innovation and Gobierno de Navarra (ADICAP; ref. IPT-2011-1717-900000). Rebeca Penalva acknowledges the “Asociación de Amigos Universidad de Navarra” for the financial support.

References

- Aherne, S.A., O'Brien, N.M., 2002. Dietary flavonols: Chemistry, food content, and metabolism. *Nutrition* 18, 75–81.
- Anand David, A., Arulmoli, R., Parasuraman, S., 2016. Overviews of biological importance of quercetin: A bioactive flavonoid. *Pharmacogn. Rev.* 10, 84. <https://doi.org/10.4103/0973-7847.194044>
- Babu, P.R., Babu, K.N., Peter, P.L.H., Rajesh, K., Babu, P.J., 2013. Influence of quercetin on the pharmacokinetics of ranolazine in rats and in vitro models. *Drug Dev. Ind. Pharm.* 39, 873–879. <https://doi.org/10.3109/03639045.2012.707209>
- Barreca, D., Bellocco, E., D'Onofrio, G., Nabavi, S., Daglia, M., Rastrelli, L., Nabavi, S., 2016. Neuroprotective effects of quercetin: from chemistry to medicine. *CNS Neurol. Disord. Drug Targets* 15, 964–975. <https://doi.org/10.2174/1871527315666160813175406>
- Buggins, T.R., Dickinson, P.A., Taylor, G., 2007. The effects of pharmaceutical excipients on drug disposition. *Adv. Drug Deliv. Rev.* 59, 1482–1503. <https://doi.org/10.1016/j.addr.2007.08.017>
- Bule, M., Abdurahman, A., Nikfar, S., Abdollahi, M., Amini, M., 2019. Antidiabetic effect of quercetin: A systematic review and meta-analysis of animal studies. *Food Chem. Toxicol.* 125, 494–502. <https://doi.org/10.1016/j.fct.2019.01.037>
- Caddeo, C., Gabriele, M., Fernández-Busquets, X., Valenti, D., Fadda, A.M., Pucci, L., Manconi, M., 2019. Antioxidant activity of quercetin in Eudragit-coated liposomes for intestinal delivery. *Int. J. Pharm.* 565, 64–69. doi: 10.1016/j.ijpharm.2019.05.007.
- Chen, I.L., Tsai, Y.J., Huang, C.M., Tsai, T.H.U., 2010. Lymphatic absorption of quercetin and rutin in rat and their pharmacokinetics in systemic plasma. *J. Agric. Food Chem.* 58, 546–551. <https://doi.org/10.1021/jf9026124>
- Chen, S., Jiang, H., Wu, X., Fang, J., 2016. Therapeutic effects of quercetin on inflammation, obesity, and type 2 diabetes. *Mediators Inflamm.* 2016, 1–5. <https://doi.org/10.1155/2016/9340637>
- Chen, X., Yin, O.Q.P., Zuo, Z., Chow, M.S.S., 2005. Pharmacokinetics and modeling of quercetin and metabolites. *Pharm. Res.* 22, 892–901. <https://doi.org/10.1007/s11095-005-4584-1>
- Costa, P., Sousa Lobo, J.M., 2001. Modeling and comparison of dissolution profiles. *Eur. J. Pharm. Sci.* 13, 123–33.
- Council of Europe, 2013. European Pharmacopoeia, 8th Edition, Volume 1, Strasbourg.
- Dajas, F., Abin-Carriquiry, J.A., Arredondo, F., Blasina, F., Echeverry, C., Martínez, M., Rivera, F., Vaamonde, L., 2015. Quercetin in brain diseases: potential and limits. *Neurochem. Int.* 89, 140–148. <https://doi.org/10.1016/j.neuint.2015.07.002>
- de Oliveira Pedro, R., Hoffmann, S., Pereira, S., Goycoolea, F.M., Schmitt, C.C., Neumann, M.G., 2018. Self-assembled amphiphilic chitosan nanoparticles for quercetin

- delivery to breast cancer cells. *Eur. J. Pharm. Biopharm.* 131, 203–210. <https://doi.org/10.1016/j.ejpb.2018.08.009>
- Dwyer, J.T., Wiemer, K.L., Dary, O., Keen, C.L., King, J.C., Miller, K.B., Philbert, M.A., Tarasuk, V., Taylor, C.L., Gaine, P.C., Jarvis, A.B., Bailey, R.L., 2015. Fortification and health: challenges and opportunities. *Adv. Nutr.* 6, 124–31. <https://doi.org/10.3945/an.114.007443>
- Egert, S., Wolfram, S., Bosy-Westphal, A., Boesch-Saadatmandi, C., Wagner, A.E., Frank, J., Rimbach, G., Mueller, M.J., 2018. Daily quercetin supplementation dose-dependently increases plasma quercetin concentrations in healthy humans. *J. Nutr.* 138, 1615–1621. <https://doi.org/10.1093/jn/138.9.1615>
- Ganesan, B., Brothersen, C., McMahan, D.J., 2014. Fortification of foods with omega-3 polyunsaturated fatty acids. *Crit. Rev. Food Sci. Nutr.* 54, 98–114. <https://doi.org/10.1080/10408398.2011.578221>
- Gao, L., Liu, G., Wang, X., Liu, F., Xu, Y., Ma, J., 2011. Preparation of a chemically stable quercetin formulation using nanosuspension technology. *Int. J. Pharm.* 404, 231–237. <https://doi.org/10.1016/j.ijpharm.2010.11.009>
- Ghosh, S., Dungdung, S.R., Chowdhury, S.T., Mandal, A.K., Sarkar, S., Ghosh, D., Das, N., 2011. Encapsulation of the flavonoid quercetin with an arsenic chelator into nanocapsules enables the simultaneous delivery of hydrophobic and hydrophilic drugs with a synergistic effect against chronic arsenic accumulation and oxidative stress. *Free Radic. Biol. Med.* 51, 1893–1902. <https://doi.org/10.1016/j.freeradbiomed.2011.08.019>
- Harwood, M., Danielewska-Nikiel, B., Borzelleca, J.F., Flamm, G.W., Williams, G.M., Lines, T.C., 2007. A critical review of the data related to the safety of quercetin and lack of evidence of in vivo toxicity, including lack of genotoxic/carcinogenic properties. *Food Chem. Toxicol.* 45, 2179–2205. <https://doi.org/10.1016/j.fct.2007.05.015>
- Hoffman, J.R., Falvo, M.J., 2004. Protein - Which is best? *J. Sport. Sci. Med.* 3, 118–130.
- Iacopetta, D., Grande, F., Caruso, A., Mordocco, R.A., Plutino, M.R., Scrivano, L., Ceramella, J., Muià, N., Saturnino, C., Puoci, F., Rosano, C., Sinicropi, M.S., 2017. New insights for the use of quercetin analogs in cancer treatment. *Future Med. Chem.* 9, 2011–2028. <https://doi.org/10.4155/fmc-2017-0118>
- Iacopini, P., Baldi, M., Storchi, P., Sebastiani, L., 2008. Catechin, epicatechin, quercetin, rutin and resveratrol in red grape: Content, in vitro antioxidant activity and interactions. *J. Food Compos. Anal.* 21, 589–598. <https://doi.org/10.1016/j.jfca.2008.03.011>
- Ishikawa, M., Yoshii, H., Furuta, T., 2005. Interaction of modified cyclodextrins with cytochrome P-450. *Biosci. Biotechnol. Biochem.* 69, 246–248. <https://doi.org/10.1271/bbb.69.246>
- Jain, A.K., Thanki, K., Jain, S., 2014. Novel self-nanoemulsifying formulation of quercetin: implications of pro-oxidant activity on the anticancer efficacy. *Nanomedicine* 10, 959–969. <https://doi.org/10.1016/j.nano.2013.12.010>
- Karadag, A., Yang, X., Ozcelik, B., Huang, Q., 2013. Optimization of preparation conditions for quercetin nanoemulsions using response surface methodology. *J. Agric. Food Chem.* 61, 2130–2139. <https://doi.org/10.1021/jf3040463>
- Karam, M.C., Gaiani, C., Hosri, C., Burgain, J., Scher, J., 2013. Effect of dairy powders fortification on yogurt textural and sensorial properties: a review. *J. Dairy Res.* 80,

- 400–409. <https://doi.org/10.1017/S0022029913000514>
- Kashyap, D., Mittal, S., Sak, K., Singhal, P., Tuli, H.S., 2016. Molecular mechanisms of action of quercetin in cancer: recent advances. *Tumor Biol.* 37, 12927–12939. <https://doi.org/10.1007/s13277-016-5184-x>
- Khaled, K.A., El-Sayed, Y.M., Al-Hadiya, B.M., 2003. Disposition of the flavonoid quercetin in rats after single intravenous and oral doses. *Drug Dev. Ind. Pharm.* 29, 397–403. <https://doi.org/10.1081/DDC-120018375>
- Kim, M.K., Park, K. su, Yeo, W. seok, Choo, H., Chong, Y., 2009. In vitro solubility, stability and permeability of novel quercetin-amino acid conjugates. *Bioorganic Med. Chem.* 17, 1164–1171. <https://doi.org/10.1016/j.bmc.2008.12.043>
- Lee, M., Fennema, O.R., 1991. Ability of cyclodextrins to inhibit aggregation of β -casein. *J. Agric. Food Chem.* 39, 17–21. <https://doi.org/10.1021/jf00001a003>
- Li, H.L., Zhao, X. Bin, Ma, Y.K., Zhai, G.X., Li, L.B., Lou, H.X., 2009. Enhancement of gastrointestinal absorption of quercetin by solid lipid nanoparticles. *J. Control. Release* 133, 238–244. <https://doi.org/10.1016/j.jconrel.2008.10.002>
- Limtrakul, P., Khantamat, O., Pintha, K., 2005. Inhibition of P-glycoprotein function and expression by kaempferol and quercetin. *J. Chemother.* 17, 86–95. <https://doi.org/10.1179/joc.2005.17.1.86>
- Lin, J., Teo, L.M., Leong, L.P., Zhou, W., 2019. In vitro bioaccessibility and bioavailability of quercetin from the quercetin-fortified bread products with reduced glycemic potential. *Food Chem.* 286, 629–635. <https://doi.org/10.1016/j.foodchem.2019.01.199>
- Lodi, F., Jimenez, R., Moreno, L., Kroon, P.A., Needs, P.W., Hughes, D.A., Santos-Buelga, C., Gonzalez-Paramas, A., Cogolludo, A., Lopez-Sepulveda, R., Duarte, J., Perez-Vizcaino, F., 2009. Glucuronidated and sulfated metabolites of the flavonoid quercetin prevent endothelial dysfunction but lack direct vasorelaxant effects in rat aorta. *Atherosclerosis* 204, 34–39. <https://doi.org/10.1016/j.atherosclerosis.2008.08.007>
- Moreno, L.C.G.E.I., Puerta, E., Suárez-Santiago, J.E., Santos-Magalhães, N.S., Ramirez, M.J., Irache, J.M., 2017. Effect of the oral administration of nanoencapsulated quercetin on a mouse model of Alzheimer’s disease. *Int. J. Pharm.* 517, 50–57. <https://doi.org/10.1016/j.ijpharm.2016.11.061>
- Murota, K., Terao, J., 2005. Quercetin appears in the lymph of unanesthetized rats as its phase II metabolites after administered into the stomach. *FEBS Lett.* 579, 5343–5346. <https://doi.org/10.1016/j.febslet.2005.08.060>
- Nakamura, T., Kinjo, C., Nakamura, Y., Kato, Y., Nishikawa, M., Hamada, M., Nakajima, N., Ikushiro, S., Murota, K., 2018. Lymphatic metabolites of quercetin after intestinal administration of quercetin-3-glucoside and its aglycone in rats. *Arch. Biochem. Biophys.* 645, 126–136. <https://doi.org/10.1016/j.abb.2018.03.024>
- Patel, R. V., Mistry, B.M., Shinde, S.K., Syed, R., Singh, V., Shin, H.S., 2018. Therapeutic potential of quercetin as a cardiovascular agent. *Eur. J. Med. Chem.* 155, 889–904. <https://doi.org/10.1016/j.ejmech.2018.06.053>
- Penalva, R., Esparza, I., Agüeros, M., Gonzalez-Navarro, C.J., Gonzalez-Ferrero, C., Irache, J.M., 2015. Casein nanoparticles as carriers for the oral delivery of folic acid. *Food Hydrocoll.* 44, 399–406. <https://doi.org/10.1016/j.foodhyd.2014.10.004>
- Peñalva, R., Morales, J., González-Navarro, C.J., Larrañeta, E., Quincoces, G., Peñuelas, I., Irache, J.M., 2018. Increased oral bioavailability of resveratrol by its

- encapsulation in casein nanoparticles. *Int. J. Mol. Sci.* 19. <https://doi.org/10.3390/ijms19092816>
- Perez-Vizcaino, F., Duarte, J., Andriantsitohaina, R., 2006. Endothelial function and cardiovascular disease: Effects of quercetin and wine polyphenols. *Free Radic. Res.* 40, 1054–1065. <https://doi.org/10.1080/10715760600823128>
- Pool, H., Quintanar, D., Figueroa, J. de D., Bechara, J.E.H., McClements, D.J., Mendoza, S., 2012. Polymeric Nanoparticles as Oral Delivery Systems for Encapsulation and Release of Polyphenolic Compounds: Impact on Quercetin Antioxidant Activity & Bioaccessibility. *Food Biophys.* 7, 276–288. <https://doi.org/10.1007/s11483-012-9266-z>
- Rauf, A., Imran, M., Khan, I.A., ur-Rehman, M., Gilani, S.A., Mehmood, Z., Mubarak, M.S., 2018. Anticancer potential of quercetin: A comprehensive review. *Phyther. Res.* 32, 2109–2130. <https://doi.org/10.1002/ptr.6155>
- Reinboth, M., Wolfram, S., Abraham, G., Ungemach, F.R., Cermak, R., 2010. Oral bioavailability of quercetin from different quercetin glycosides in dogs. *Br. J. Nutr.* 104, 198–203. <https://doi.org/10.1017/S000711451000053X>
- Rinwa, P., Kumar, A., 2017. Quercetin along with piperine prevents cognitive dysfunction, oxidative stress and neuro-inflammation associated with mouse model of chronic unpredictable stress. *Arch. Pharm. Res.* 40, 1166–1175. <https://doi.org/10.1007/s12272-013-0205-4>
- Ritger, P.L., Peppas, N.A., 1987. A simple equation for description of solute release I. Fickian and non-Fickian release from non-swellable devices in the form of slabs, spheres, cylinders or discs. *J. Control. Release* 5, 23–36. [https://doi.org/10.1016/0168-3659\(87\)90034-4](https://doi.org/10.1016/0168-3659(87)90034-4)
- Russo, M., Spagnuolo, C., Tedesco, I., Bilotto, S., Russo, G.L., 2012. The flavonoid quercetin in disease prevention and therapy: facts and fancies. *Biochem. Pharmacol.* 83, 6–15. <https://doi.org/10.1016/j.bcp.2011.08.010>
- Scalia, S., Mezzena, M., 2009. Incorporation of quercetin in lipid microparticles: Effect on photo- and chemical-stability. *J. Pharm. Biomed. Anal.* 49, 90–94. <https://doi.org/10.1016/j.jpba.2008.10.011>
- Serno, T., Geidobler, R., Winter, G., 2011. Protein stabilization by cyclodextrins in the liquid and dried state. *Adv. Drug Deliv. Rev.* 63, 1086–1106. <https://doi.org/10.1016/j.addr.2011.08.003>
- Smith, A.J., Kavuru, P., Wojtas, L., Zaworotko, M.J., Shytle, R.D., 2011. Cocrystals of quercetin with improved solubility and oral bioavailability. *Mol. Pharm.* 8, 1867–1876. <https://doi.org/10.1021/mp200209j>
- Takizawa, Y., Kishimoto, H., Nakagawa, M., Sakamoto, N., Tobe, Y., Furuya, T., Tomita, M., Hayashi, M., 2013. Effects of pharmaceutical excipients on membrane permeability in rat small intestine. *Int. J. Pharm.* 453, 363–370. <https://doi.org/10.1016/j.ijpharm.2013.05.055>
- Wang, X., Chen, Y., Dahmani, F.Z., Yin, L., Zhou, J., Yao, J., 2014. Amphiphilic carboxymethyl chitosan-quercetin conjugate with P-gp inhibitory properties for oral delivery of paclitaxel. *Biomaterials* 35, 7654–7665. <https://doi.org/10.1016/j.biomaterials.2014.05.053>
- Zhang, M., Swarts, S.G., Yin, L., Liu, C., Tian, Y., Cao, Y., Swarts, M., Yang, S., Zhang, S.B., Zhang, K., Ju, S., Olek Jr., D.J., Schwartz, L., Keng, P.C., Howell, R., Zhang, L., Okunieff, P., 2011. Antioxidant properties of quercetin. *Adv. Exp. Med. Biol.* 701,

283-289. https://doi.org/10.1007/978-1-4419-7756-4_38

Zhang, Y., Meng, F.C., Cui, Y.L., Song, Y.F., 2011. Enhancing effect of hydroxypropyl- β -cyclodextrin on the intestinal absorption process of genipin. *J. Agric. Food Chem.* 59, 10919–10926. <https://doi.org/10.1021/jf202712y>

Figure captions

Figure 1. Influence of the incubation time (15, 30 and 60 min) and the quercetin-to-HP- β -CD ratio (1:1, 1:2 and 1:3 by mol) on the flavonoid loading (line, left axis) and its encapsulation efficiency (bars, right axis). Data are expressed as the mean \pm SD, n=3.

Figure 2. Scanning electron microscopy (SEM) of casein nanoparticles. (A) Q-NP: quercetin-loaded casein nanoparticles; (B) Q-HPCD-NP: quercetin-loaded casein nanoparticles containing hydroxypropyl- β -cyclodextrin.

Figure 3. In vitro release studies of quercetin-loaded in nanoparticles. Q-NP: quercetin-loaded casein nanoparticles; Q-HPCD-NP: quercetin-loaded in casein nanoparticles containing HP- β -CD. Data are expressed as the mean \pm SD, (n=3).

Figure 4. Quercetin plasma concentration vs. time after the oral administration of the different formulations at a dose of 25 mg/kg. Q-susp: quercetin aqueous suspension; Q-sol: quercetin solution in a PEG400-water mixture; Q-NP: quercetin-loaded casein nanoparticles; Q-HPCD-NP: quercetin-loaded casein nanoparticles in the presence of HP- β -CD. Data are expressed as mean \pm SD (n=6).

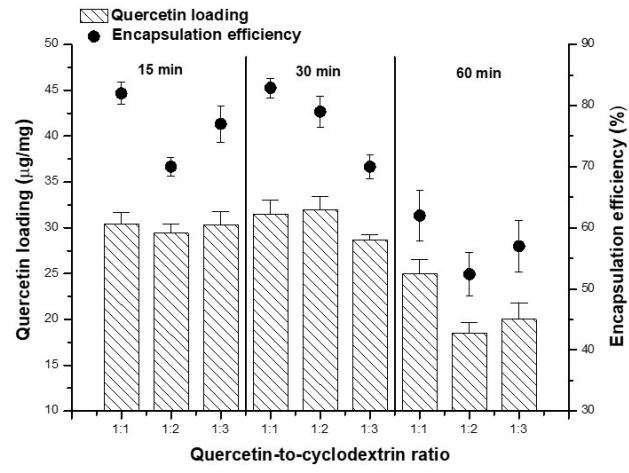


Figure 1

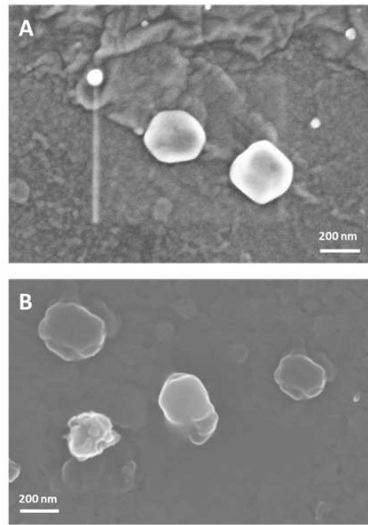


Figure 2

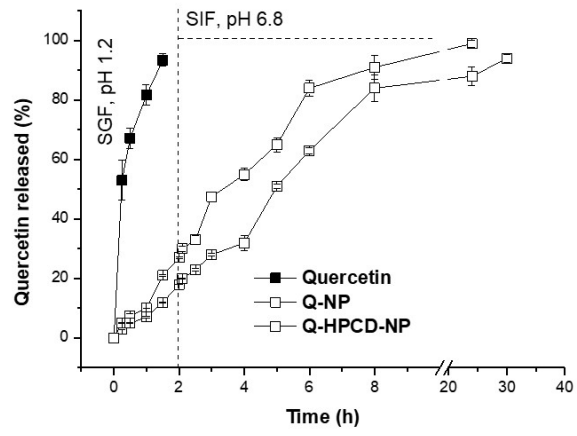


Figure 3

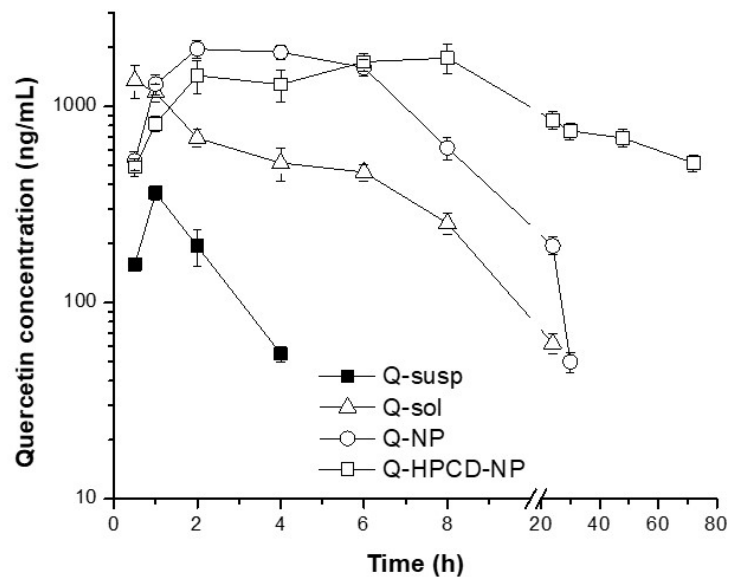


Figure 4

Table 1. Physico-chemical characteristics of empty (NP and HPCD-NP) and quercetin-loaded nanoparticles (Q-NP and Q-HPCD-NP). Data are expressed as the mean \pm SD, (n=3).

Formulation	Size (nm)	PDI	Zeta potential (mV)	Quercetin loading ($\mu\text{g}/\text{mg}$)	E.E. (%)
NP	138 \pm 13	0.19 \pm 0.02	-11.9 \pm 0.9	-	-
HPCD-NP	141 \pm 3	0.17 \pm 0.01	-12.3 \pm 2.1	-	-
Q-NP	251 \pm 9	0.26 \pm 0.02	-14.3 \pm 1.1	22.3 \pm 0.3	75.4 \pm 0.9
Q-HPCD-NP	171 \pm 5	0.19 \pm 0.01	-15.2 \pm 1.1	31.5 \pm 1.8	82.9 \pm 3.1

Table 2. Analysis of quercetin release from casein nanoparticles when incubated during the first two hours in SGF and, then, in SIF.

	Korsmeyer-Peppas			Zero-Order	
	K_{KP} (h⁻ⁿ)	n	R²	K_{ZO} (h⁻¹)	R²
Q-NP	0.14±0.01	0.94±0.06	0.983	0.13±0.01	0.982
Q-HPCD-NP	0.10±0.01	1.02±0.06	0.986	0.10±0.01	0.985

Table 3. Pharmacokinetic parameters of quercetin calculated from either the intravenous or oral administration of a single dose of the flavonoid (25 mg/Kg) formulated as a solution, suspension or encapsulated in nanoparticles. Q-IV. Quercetin intravenous solution in a mixture of PEG400 and water; Q-susp: quercetin aqueous suspension; Q-sol: oral quercetin solution in a mixture of PEG400 and water; Q-NP: quercetin-loaded casein nanoparticles; Q-HPCD-NP: quercetin-loaded casein nanoparticles in the presence of HP- β -CD. Data are expressed as the mean \pm SD; (n=6).

	T_{max} (h)	C_{max} (μg/mL)	t_{1/2} (h)	AUC (μg h/mL)	V (mL)	Cl (mL/h)	MRT (h)	F (%)
Q-IV	0.0 \pm 0.0	176 \pm 13.4	0.60 \pm 0.35	167 \pm 8.21	26.3 \pm 16.1	30.2 \pm 1.35	1.57 \pm 0.12	100
Q-susp	1.0 \pm 0.0	0.37 \pm 0.08**	0.54 \pm 0.49**	0.55 \pm 0.25**	29.1 \pm 24.5**	45.3 \pm 19.0	1.22 \pm 0.35**	0.33
Q-sol	0.60 \pm 0.22	1.40 \pm 0.41	3.51 \pm 1.97	6.77 \pm 2.20	146 \pm 78.9	29.2 \pm 0.91	4.86 \pm 0.55	4.10
Q-NP	3.7 \pm 1.5**	2.20 \pm 0.40*	6.28 \pm 1.51*	19.6 \pm 4.12**	262 \pm 60.9**	29.0 \pm 0.92	7.78 \pm 1.68**	11.8
Q-HPCD-NP	6.3 \pm 2.7**	1.89 \pm 1.05	28.41 \pm 7.35**+	61.4 \pm 24.5**+	893 \pm 137**+	22.3 \pm 2.61	28.5 \pm 3.01**+	36.8

C_{max}: peak plasma concentration; T_{max}: time to reach plasma concentration; AUC: Area under the curve; t_{1/2}: half life of the terminal phase; V: Volume of distribution, Cl: Clearance; MRT: mean residence time Fr: relative oral bioavailability

* Significant differences vs Q-sol (p<0.05) Mann-Whitney-U

** Significant differences vs Q-sol (p<0.01) Mann-Whitney-U

+ Significant differences vs Q-NP (p<0.01) Mann-Whitney-U

